Ultramicrostructure and Microthermomechanics of Biological IR Detectors: Materials Properties from a Biomimetic Perspective

J. Hazel,[†] N. Fuchigami,[‡] V. Gorbunov,[‡] H. Schmitz,[§] M. Stone,[||] and V. V. Tsukruk*[,‡]

Materials Science & Engineering Program, Western Michigan University, Kalamazoo, Michigan 49008; Department of Material Science & Engineering, Iowa State University, Ames, Iowa 50011; Zoologisches Institut, Universität Bonn, Poppelsdorfer Schloss, D-53115, Bonn, Germany; Materials and Manufacturing Directorate, Air Force Research Laboratory/MLPJ, Wright-Patterson AFB, Ohio 45433

Received December 6, 2000; Revised Manuscript Received January 18, 2001

Microstructural organization of the biological infrared (IR) receptors was studied to elucidate their materials properties useful for prospective biomimetic design of artificial IR sensors from organic/polymeric materials. The IR receptors in *Melanophila acuminata* beetles were studied with ultrahigh-resolution scanning probe microscopy (SPM) in a range of temperatures. By application of micromechanical mapping and thermal stage, we made attempts to reveal the micromechanical and thermomechanical properties of the cuticular apparatus of the IR sensillum. The main component of the cuticular apparatus is an internal endocuticular sphere with a diameter of about 15−20 μm. Highly ordered multilayered organization of the lamellated peripheral mantle of the sphere was confirmed and characterized. We observed that the interlayer spacing of this microstructure varied along the circumference and decreased to 300 nm in the vertex of the sphere. We demonstrated that the microlayered structure is composed of nanolayers with very different micromechanical properties and thermal behaviors. Thermal expansion of the outer mantle was observed, and the local thermal expansion coefficient under given preparation conditions was estimated to be below 1.5×10^{-4} grad^{-1}.

Introduction

The bioinspired design of sensor devices is considered to be an intriguing venue in biomimetics. Key issues in this design optimization depend on what type of performance is going to be replicated in an artificial analogue. Very frequently, unique materials microstructure and corresponding properties are targeted in such an approach. Therefore, understanding of biological materials microstructural organization and its relationship to targeted performance from the perspective of sophisticated materials science and engineering should be the first step in this type of biomimetic research. Here, we reveal first results of our research focused on finding the prospective microstructural design for the artificial thermal sensors from organic/polymeric materials based on known natural examples.

Melanophila acuminata beetles are capable of distant detection of forest fires via paired thoracic IR pit organs.[1] A great deal of efforts were devoted to studies of beetle behavior under external IR stimuli and their physiological responses.[2−4] These behavioral and physiological studies have shown that the pit organs are most sensitive to IR radiation in the wavelength range between 2 and 4 μm.[2,3] In behavioral experiments, a radiation intensity of only 60 μW/cm^2 at the wavelength of 3 μm was sufficient to elicit a fast response in the beetle behavior.[2] On the other hand, a unique microstructural organization has been revealed by application of transmission electron microscopy (TEM). TEM studies showed that the main component of the cuticular apparatus of a single sensillum is a massive endocuticular sphere, which is placed in an internal cavity under a thin cuticular dome (Figure 1).[4] The sphere, filled with soft matter such as water and wax, is innervated from below by the sensory dendrite of a single mechanoreceptor. The dendritic tip of the mechanosensory cell is anchored in the periphery of the internal sphere where the cuticle displays numerous lamellae (Figure 1). These receptors are arranged in two-dimensional arrays of 50−100 IR sensilla located in deep pit areas (Figure 2).

According to the hypothesis of the photomechanical IR sensing of these biological receptors,[3] IR absorption in the sphere causes the cuticle to expand. The very nature of this expansion is speculated to be thermal. In a hitherto unknown way, this expansion should result in a cross compression of the dendritic tip. As is speculated, a cross compression of the dendritic tip of a mechanoreceptive sensory cell of at least 0.1 nm is necessary to stimulate the generation of action potentials in a sensitive insect mechanoreceptor.[5−7] A theoretical calculation yielded the result that a thermal expansion coefficient of 2×10^{-4} K has to be postulated to achieve this compression at a radiation intensity of 5 mW/cm^2.[2,3]

In this paper, we focus on investigation of the microstructure and microthermomechanical properties of materials that constitutes the biological IR receptors from a biomimetic

* To whom correspondence should be addressed. E-mail: vladimir@iastate.edu.

[†] Western Michigan University.

[‡] Iowa State University.

[§] Universität Bonn.

[||] Air Force Research Laboratory.

10.1021/bm005648i CCC: $20.00
Published on Web 02/10/2001

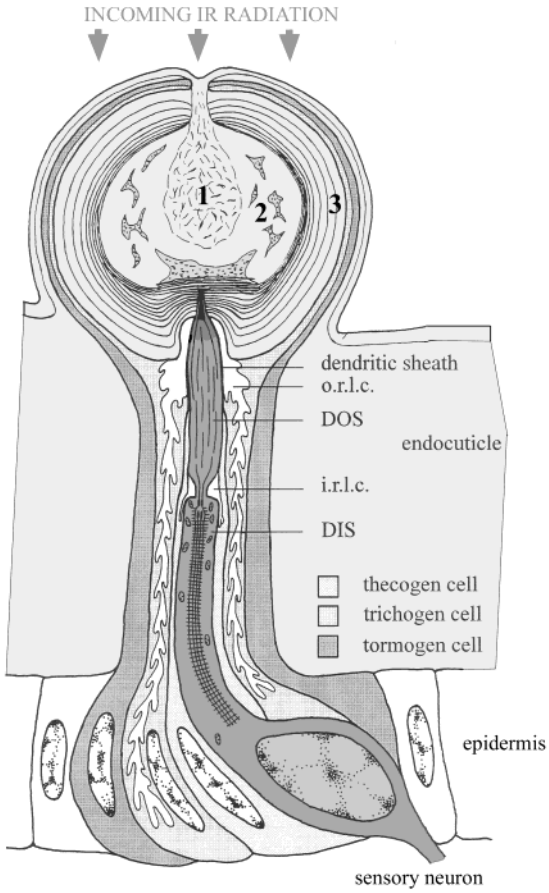

Figure 1. Schematic drawing of the IR sensillum. The internal cuticular sphere is composed of three distinguishable areas (1−3) and covered by a thin outer cuticle. Three enveloping cells (theco-, tricho-, and tormogen cell) surround the sensory neuron which is anchored with the tip of the dendrite within the peripheral area 3. Key: DIS, dendritic inner segment; DOS, dendritic outer segment; irlc, inner receptor lymph cavity; orlc, outer receptor lymph cavity. Diameter of the sphere is about 12 μm. Adapted from ref 4.

standpoint. We report on some fine peculiarities of the microstructural organization of the IR receptors in *M. acuminata* beetles, which can be useful in a prospective design of the biomimetic receptors from organic/polymeric materials based on photomechanical principles. In this study, we apply ultrahigh-resolution scanning probe microscopy (SPM), which allows direct probing of surface topography and interfacial properties by tiny SPM probes with nanoscale resolution. We attempt to reveal the micromechanical and thermomechanical properties of the receptor material by using microprobing analysis and scanning thermal microscopy (SThM) as well. This current attempt is limited to biological tissue samples obtained by conventional microtoming and fixing procedures.

Experimental Section

The pit organs were excised in iced 0.05 M cacodylate buffer with 3% glutaraldehyde (pH 7.2) and fixed for 24 h at 4 °C. After postfixation with 1.5% OsO_4 in the same buffer for 2 h and washing in buffer solution, the specimens were dehydrated in an ascending series of ethanol and embedded in Epon 812 (Luft 1961). Epon 812 is a glycid ether (i.e. the epoxypropyl ether of glycerine). The resin was hardened

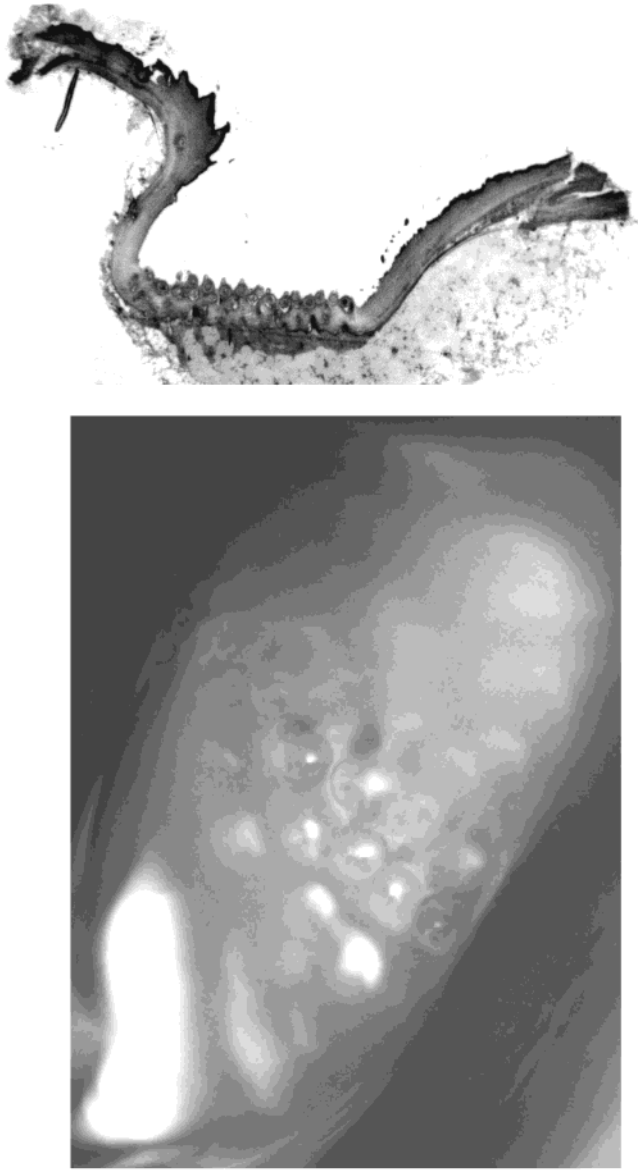

Figure 2. Optical micrograph of a section through an IR organ (top) and reflection optical micrograph of IR receptors in alive beetle (bottom). At the bottom of the pit organ, a field of about 70−100 IR sensilla is situated.

with two different hardeners: (i) DBA (2-dodecenylamberacid anhydride and (ii) MNA (methylendomethylphthalacid anhydride). We used two different mixtures named A (primarily soft) and B (primarily hard): A, Epon 812 (62 g) and hardener DBA (100 g); B, Epon 812 (100 g) and hardener MNA (89 g). A and B were mixed 7:3. During mixing, 1.5% accelerator DMP-30 was added (2,4,6-tri-(dimethylaminomethyl)phenol). Semithin sections were made with a Reichert Ultracut microtome using glass knifes.

SPM studies were performed on a Dimension 3000 (Digital Instruments, Inc.) microscope and an Explorer (Thermomicroscopes, Inc.) microscope with a scanning thermal microscopy (SThM) mode according to the procedure described in previous publications.[8,9] To reveal surface topography, we used contact and tapping modes. Surface composition was tested with lateral force mode and phase imaging. Microscopic elastic response and surface distribution of adhesion were obtained from force−distance data.[10,11]

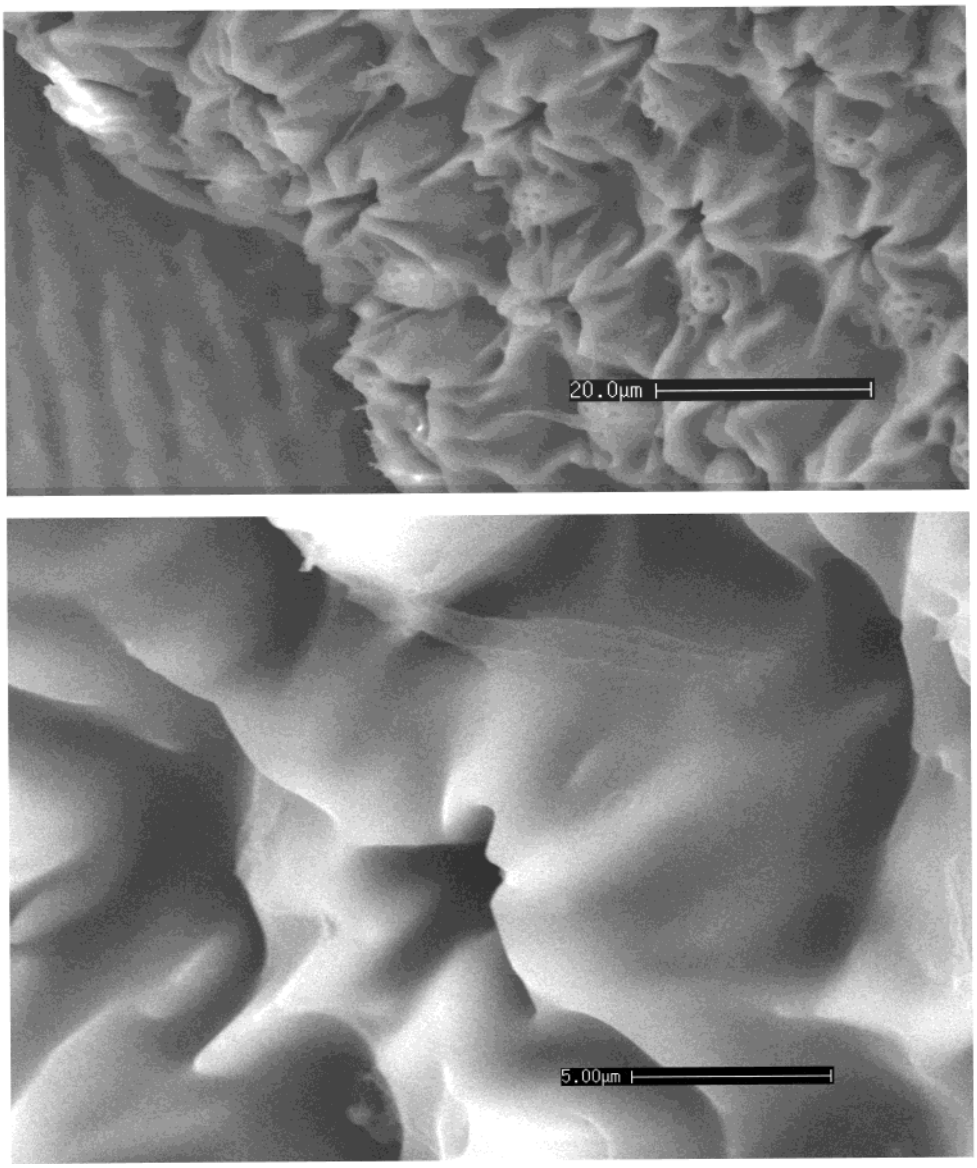

Figure 3. SEM micrographs of the receptor array after the drying procedure at different magnifications.

Surface distribution of elastic modulus was obtained in the Hertzian approximation according to our earlier developments.[10] The force−distance data were collected within selected surface areas in force−volume mode and processed to obtain histograms of the elastic modulus and adhesive force distribution.[12,13] For microthermal studies, samples were placed on a thermal stage and scanned at elevated temperatures. Heating was done step-by-step with equilibration time at each temperature of about 15 min. Surface distribution of thermal conductivity was recorded with SThM.[14,15]

Results and Discussion

A high-resolution optical micrograph of the IR organ (Figure 2) shows a distribution of spherical receptors on the bottom of the pit surface. All sensillae are very round and highly reflected spheres of about 15−20 μm micrometers in a diameter. Up to 100−150 receptors are located within a single pit area in relatively ordered manner and with dense packing. Scanning electron microscopy (SEM) micrographs of the pit areas after gentle drying process in a vacuum revealed a very different pattern. Initially very round and smooth spherical receptors adopt a collapsed shape with a central opening (Figure 3). Obviously that the walls of spherical receptors collapsed toward the center of the receptors due to removal of water and wax (their presence was indicated in recent TEM studies[4]) from inside of these receptors as a result of the drying procedure.

To reveal fine microstructure of the receptor walls, we turned to the microtomed sections of epoxy-embedded receptors prepared as described above. We used an optical system to locate a single receptor cross section and positioned the SPM tip on the selected receptor for high-resolution imaging. General overview imaging (20−50 μm across) of receptor cross sections demonstrated all major features described before on a basis of electron microscopy data (Figure 4).[4] It showed the layered microstructure of the outer areas that are slightly elevated. The central part of the sphere was much more homogeneous and possesses some depletion in the very center of the receptor.

For high-resolution imaging, we concentrated on the lamellated area of the sphere. The peripheral area shows the

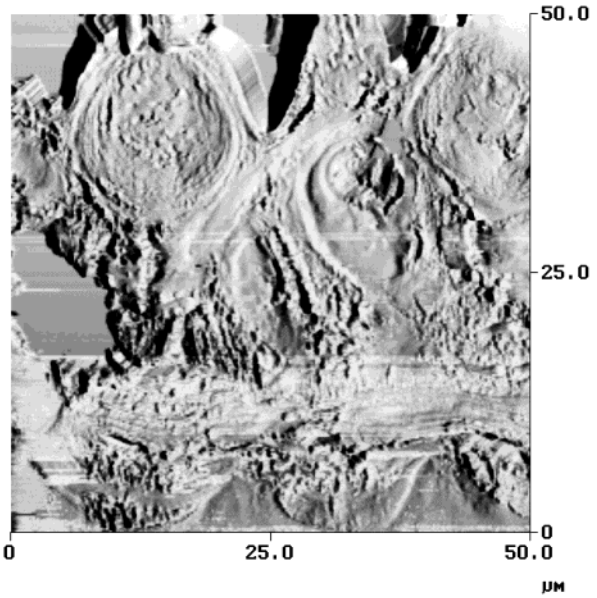

Figure 4. SPM topographical image of microtomed ultrathin slices of the receptor areas at low magnifications.

lamellated structure typical for endocuticle[16,17] (Figure 5). Up to 5−10 curved layers are densely packed and their spatial arrangements are closely correlated, as is concluded from the presence of distinctive 2-D Fourier components (not shown). Interlayer distance varies along the perimeter as demonstrated in Figure 5. The average periodicity is 300 ± 100 nm in the vicinity of the apex. This periodicity increases to 1 μm in the bottom part of receptors. Multilayered structure in the areas close to the receptor tip, consists of wide elevated strips separated by sharp deep grooves, which occupy less than 10% of the radial dimension. For multilayered structures with larger periodicity, the ridges are separated by wide valleys (Figure 5).

A new feature of surface morphology revealed by high-resolution SPM scanning was the presence of ultrafine grain texture (Figures 5 and 6). The lateral grain dimensions were in the range 50−150 nm. The grains had irregular shape and were separated by sharp microcracks, as can be seen from higher resolution "deflection" mode that emphasizes fine details by removing a "height" contribution in the topographical image (Figure 6). Lateral force microscopy clearly showed grainy texture with groove and grain edges emphasized by spikes in the lateral forces (Figure 5). These variations are, to some extent, caused by a "geometrical" contribution generated by the steep edges of microcracks and ridges.[18]

As is known, the surface variation of the lateral forces in the contact mode and the phase shift in the tapping mode are determined by the surface distribution of the shear strength and viscoelasticity/adhesion, respectively.[18,19] These properties correlate closely with chemical composition and local stiffness of the surface. Therefore, these modes are considered to be instructive for testing surface composition. Both lateral force (Figure 5) and phase (Figure 7) images demonstrate that the surface of receptor cross sections is relatively homogeneous without significant variation of local chemical composition and stiffness. On top of the ridges, lateral force fluctuations are reduced. Significant increase of the lateral forces is observed along the groove edges and along the edges of grainy texture (Figure 5). The asymmetric shape of the lateral force response indicates significant contribution from "geometrical" friction caused by tilt of the SPM tip climbing over steep edges.

Pixel-by-pixel micromapping of the micromechanical properties revealed the variation of local elastic response and adhesive forces associated with multilayered structure.[13,19,20] Elastic deformation was probed up to the indentation depth of 10−20 nm. Under these conditions, the surface was deformed elastically and was fully recoverable. The surface elasticity possessed a very broad distribution with higher modulus values on top of the grains and lower elastic modulus within the grooves (Figure 8). Surface distribution histograms possessed a peak value around 1.3 GPa and a mean value close to 3 GPa (Figure 8). These values were similar to expected elastic moduli value for the outer areas of insects.[21] Surface distribution of elastic modulus was broad due to variable contributions from surface areas within grooves and the tops of grainy ridges. In some places, indications of very thin topmost surface layer were detected that can be related to some surface contamination related to the microtoming procedure (see below). However, the estimated thickness of these layers did not exceed several nanometers, and their presence did not affect measured elastic and adhesive properties. The adhesive force distribution closely followed topography and showed lower values along the main grooves with higher values on top of the grainy-textured surface (Figure 9). This surface distribution correlated well with the uneven distribution of elastic modulus and resulted in a bimodal surface distribution of adhesive forces with higher adhesion detected within between grains (Figure 9).

Therefore, surface micromapping confirmed variable elastic and adhesive properties of the multilayered peripheral area. Significant variation of surface micromechanical properties can be associated with the lamellated endocuticular structure typical for insect cuticle as known from TEM experiments.[20] Insect cuticle is composed of microscopic fibrils organized in layers with alternating orientations in perpendicular directions along the surface.[21] In such a case, microtoming exposes fibrils cut either in transversal or longitudinal directions. These cross sections will have very different micromechanical properties due to their natural anisotropy of fiber cross sections.

Here, we need to mention that the standard procedure of the embedment of biological material into a polymeric matrix (epoxy resins) to provide support for microtoming may result in a number of artifacts unnoticed by the SEM technique but critical for SPM imaging. This is due to the fact that SPM scanning involves direct physical contact of the nanosharp tip and the surface. Surface contamination due to the transfer of a thin layer of polymeric materials onto the sliced surface during the cutting procedure can be an issue for measuring fine surface details. However, epoxy resin material has a high glass transition temperature (>100 °C) after curing at elevated temperature. This significantly reduces the polymer mobility (even at elevated temperature) and should prevent its transfer to the inner surface. Indeed,

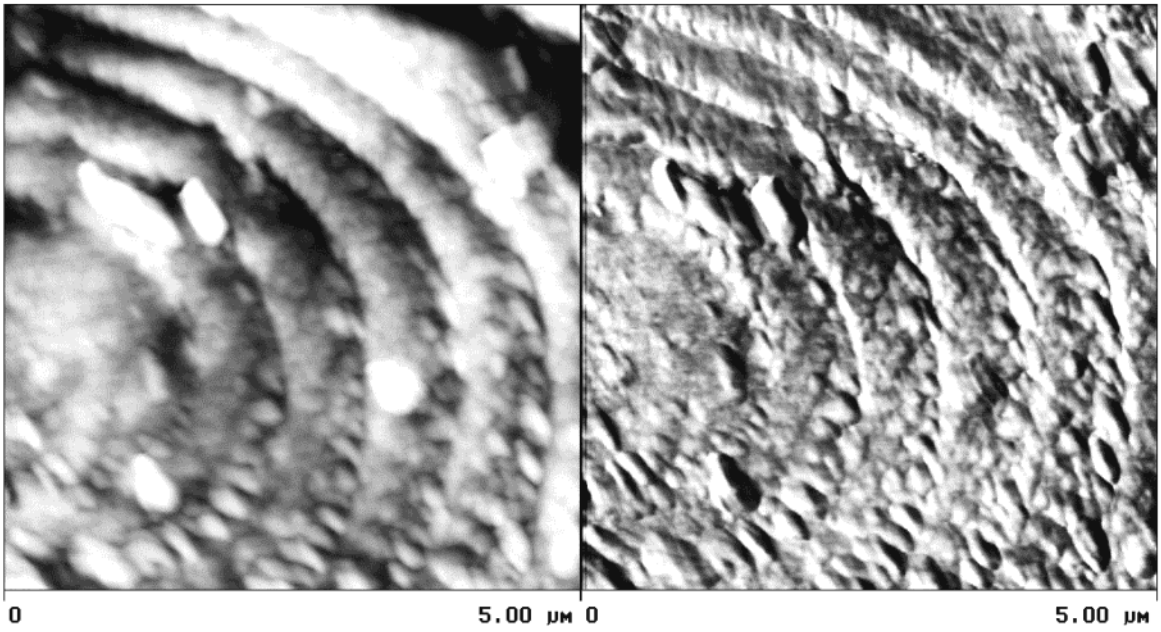

Figure 5. SPM topography (left) and lateral force (right) images of multilayered structures in outer areas of IR receptors at intermediate magnifications.

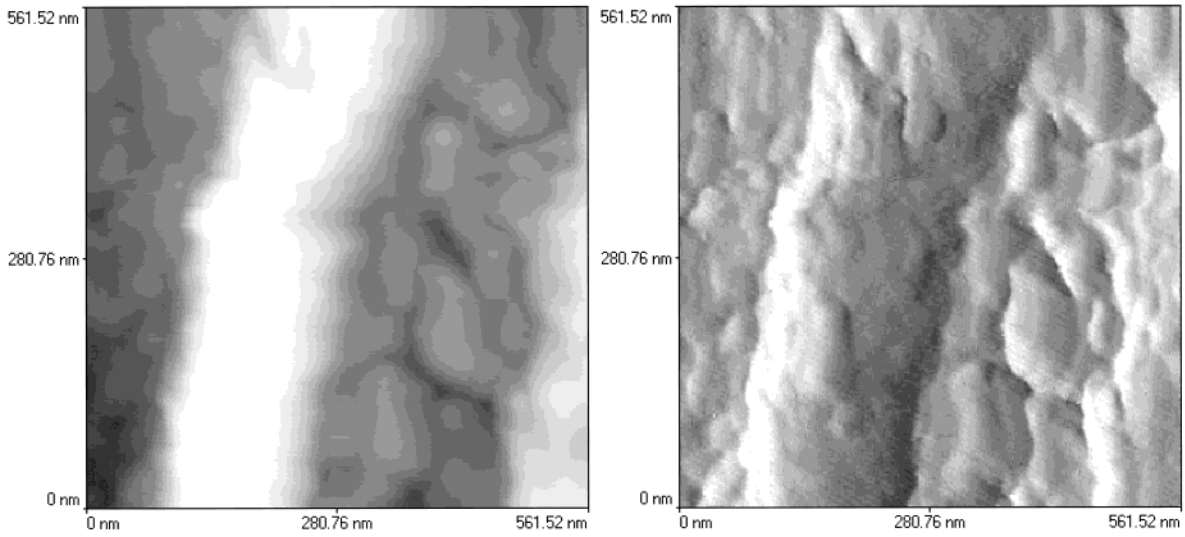

Figure 6. SPM topography (left) and amplitude deflection (right) images of multilayered structures with fine grainy morphology at highest magnifications.

the quality of ultrahigh resolution images (sharpness, edges) confirms that a surface film, if present, could not be thicker than several nanometers. The presence of such ultrathin surface film should not significantly affect our morphology and micromechanical measurements. However, the thermal expansion of original material can be limited by the thermal properties of the epoxy matrix.

As the next step, we studied the thermal behavior of the peripheral area. Before these measurements, we tested if the epoxy resin surface film could significantly affect our results. For this, we probed the surface of epoxy resin outside of the receptor areas. As we observed, the surface stiffness of epoxy resin was high and greatly exceeded 2−3 GPa. This confirms that the resin is in glassy state after curing. We observed that a small fraction of the resin surface became more compliant at temperatures above 95 °C. This can be related to the beginning of the glass transition. Therefore, to avoid significant contribution from possible softening of the surface resin film, we limited our measurements to temperatures below 95 °C.

SThM imaging shows concurrently obtained surface distributions of topography and local heat dissipation associated with thermal conductivity (Figure 10).[14] Because of the shape of the thermal probe with an effective radius of 5 μm, the spatial topographical resolution of this mode was limited to several tenths of a micrometer. Therefore, we did not expect to visualize all of the fine details of the IR receptors (like multilayered structures) in this mode and instead focused on micrometer scale features revealed by SThM.

First, very close correlation was observed between surface topography and the thermal signal (Figure 10). In the areas of the receptor tip and receptor bottom, significant depletion was observed and multilayered edges (microstructure is not

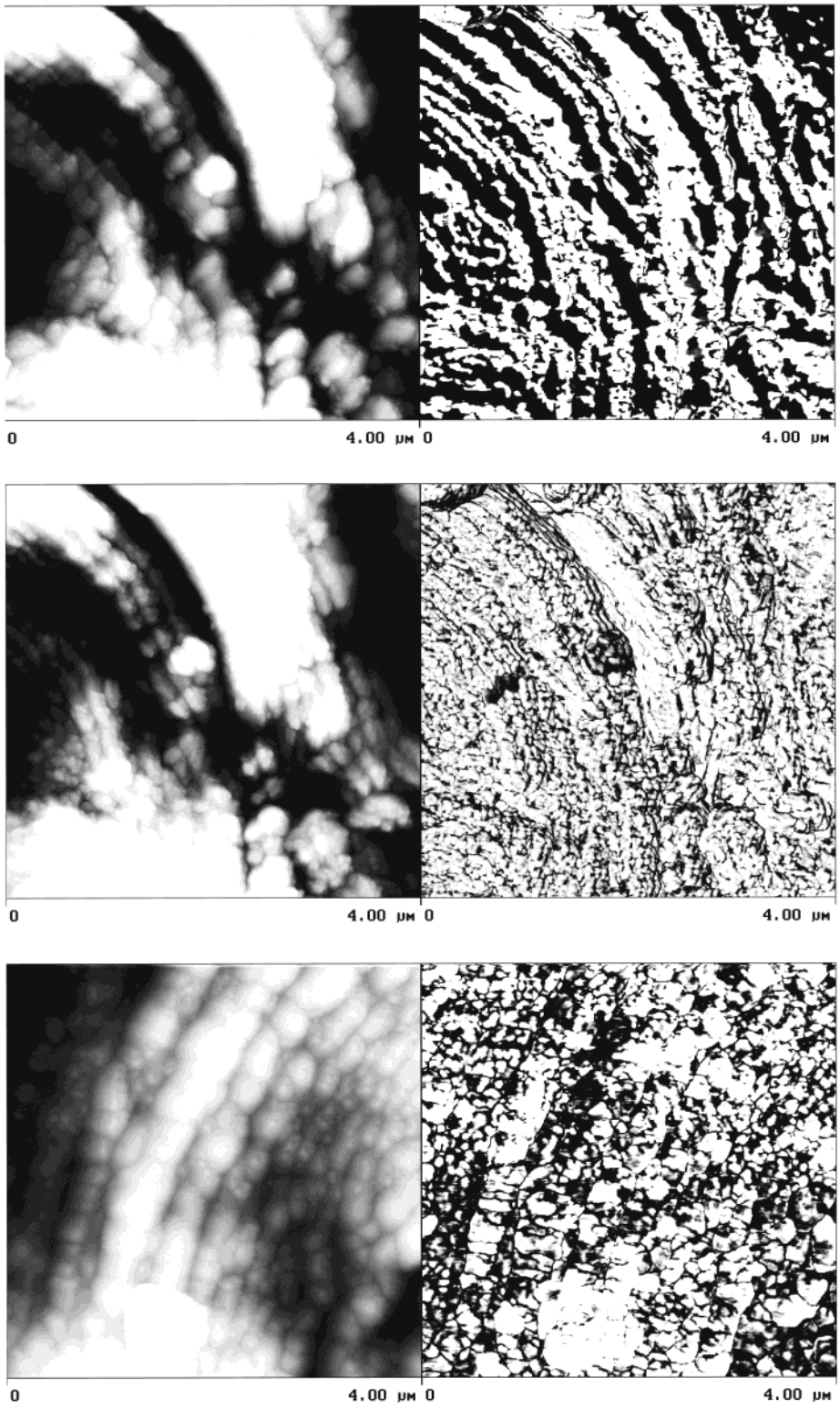

Figure 7. SPM topography (left) and phase (right) images of multilayered structures in outer areas of IR receptors at different temperatures: bottom, 25 °C; middle, 50 °C; top, 70 °C.

visible in this mode) were elevated. Heat dissipation detected simultaneously with topography recording was much higher than the background level for depletions in both the tip and bottom areas (Figure 10). The lowest heat dissipation was observed along the elevated peripheral area. Obviously, the surface distribution of heat dissipation is affected by the variation of the tip−surface contact area caused by topography. Because of obvious geometrical reasons, in depleted parts of receptors, the contact area increases, and along the ridges, the contact area decreases. This should result in corresponding increasing and decreasing of the integrated heat dissipation even if actual local thermal conductivity is unchanged. Because of very complicated tip−curved surface interactions, separation of these contributions cannot be done in a simple analytical or numerical way. At this stage of the development of this experimental technique, we cannot

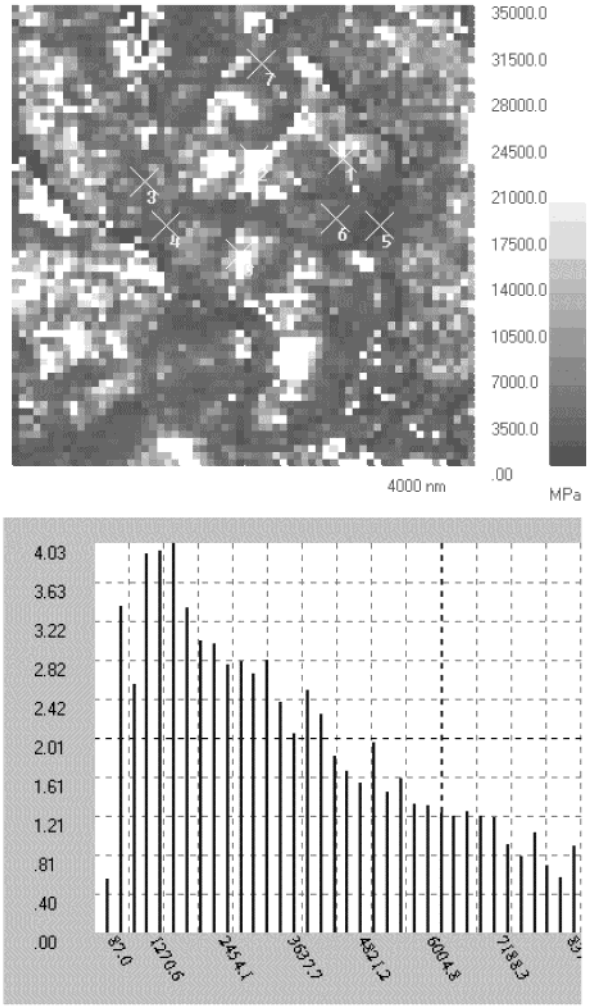

Figure 8. Micromapping of elastic modulus (32 × 32 pixels, 4 × 4 μm) (top) and corresponding surface histogram distribution of elastic modulus (bottom).

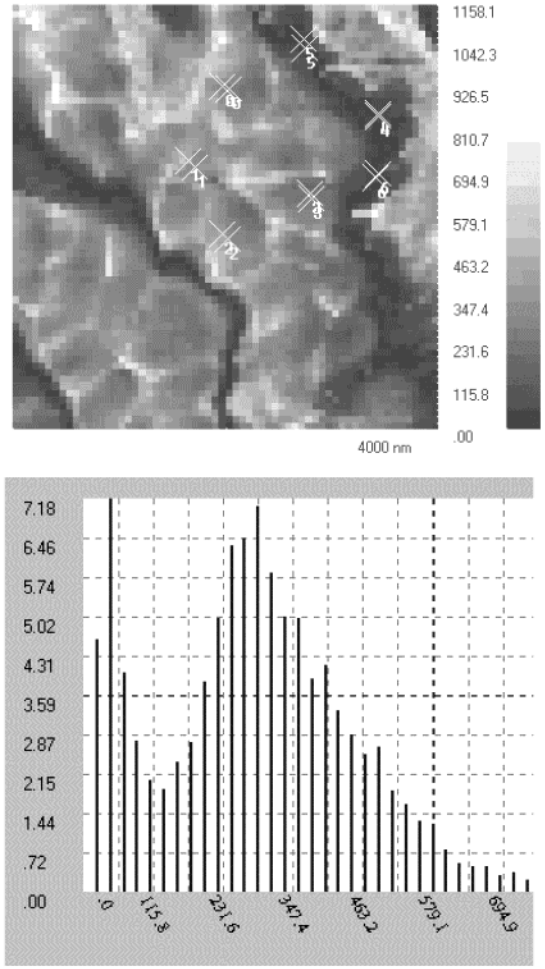

Figure 9. Micromapping of adhesive forces (32 × 32 pixels, 4 × 4 μm) (top) and corresponding surface histogram distribution of adhesive forces (bottom).

quantify this observation nor evaluate what fraction of heat dissipation variation is related to microstructure/materials properties. Further investigations with higher resolution and the development of quantitative models of heat dissipation through the tip−surface interface are required to deconvolute topographical and thermal contributions.

Finally, we tested multilayered microstructure of the IR receptors at elevated temperatures (Figure 7). Samples were heated by 5−10 °C and equilibrated, and SPM images were taken from the same surface area at identical scanning conditions. As is clear from these images, the multilayered structure undergoes significant changes during heating. Although surface topography remained virtually unchanged, phase images were changed completely at elevated temperature. Heating to intermediate temperatures (40−60 °C) led to a significant increase of dark areas on the phase images (Figure 7). Further heating resulted in dramatic changes of the phase image: clear layering occurred with the formation of a very distinctive multilayered pattern that exhibited large differences in the phase shift between adjacent layers (Figure 7). This change demonstrated that softening of the multilayered structure occurred nonuniformly, with interlayers becoming compliant at elevated temperature. This observation is a confirmation of the fact that layers in the peripheral area of the sphere are composed from materials with different mechanical and thermal properties.

By scanning silicon grids in the same range of temperatures, we observed that, despite thermal drifts, lateral dimensions of surface features on SPM images obtained at elevated temperatures, can be reproduced within ±0.5%. Thus, topography data can be used for evaluation of the rate of thermal expansion. To improve accuracy of dimensional measurements, we used an image analysis procedure to enhance grain boundaries. The variation of the interlayer periodicity averaged over three independent measurements for two independent heating cycles is presented in Figure 11. From these data it is clear that very minor thermal expansion of the multilayered structure occurred during heating from 25 to 95 °C. Linear regression analysis of the data gave a thermal expansion coefficient of $k = 1.5 \times 10^{-4}$ grad^{-1}. If only the temperature interval below 90 °C is included in the analysis, the measured value of the thermal expansion coefficient drops by 50%. The uncertainty of our measurements of interlayer spacing prevented more precise estimation. Therefore, we can conclude that the thermal expansion coefficient of multilayered structure as estimated under given conditions does not exceed 1.5×10^{-4} grad^{-1}. It is worth noting that the current estimation represents thermal expansion for material embedded in an epoxy matrix.

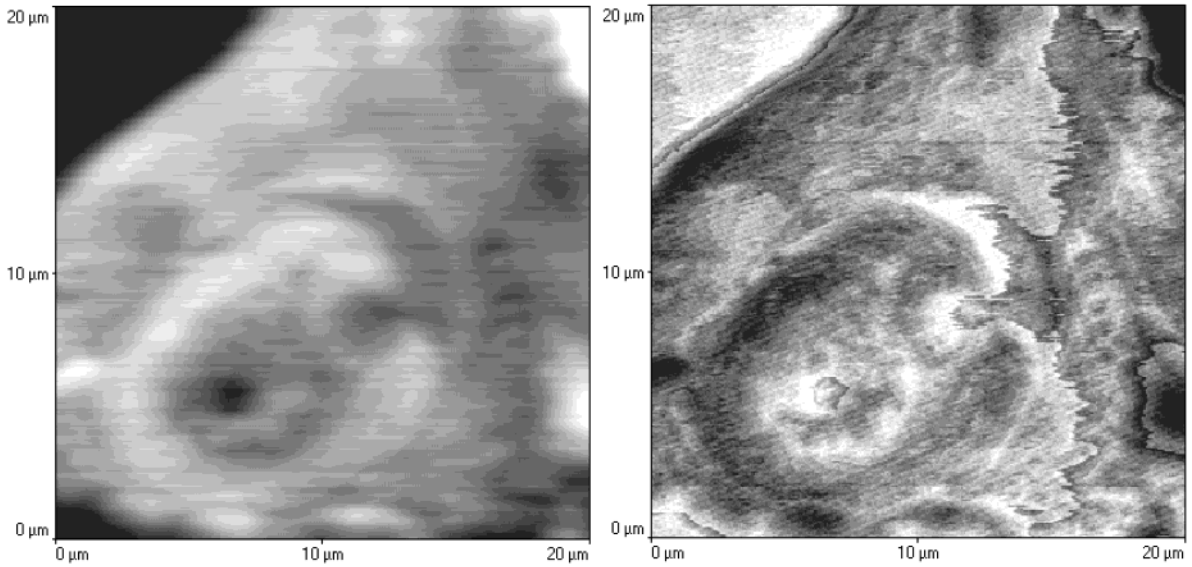

Figure 10. SThM topography (left) and heat dissipation (right) images of a section of the IR receptor.

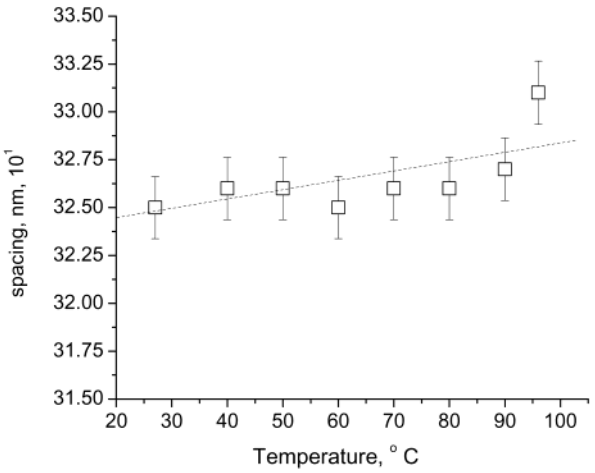

Figure 11. Temperature variation of multilayered spacing for sections of the IR receptors during the heating cycle.

Conclusions and Prospectives

SPM studies of beetle IR sensilla revealed several ultrafine features of their cuticular apparatus. First, we confirmed previous electron microscopic data on the structure of the peripheral lamellated area of the internal sphere composed of alternating elevated layers and grooves with layered periodicity in the range 0.3−1.0 μm and correlated packing of 5−10 layers. Second, ultrahigh-resolution imaging revealed nanograiny surface texture with irregular grains of 50−150 nm, densely packed along the perimeter and separated by grooves and microcracks. Third, scanning thermal microscopy showed much higher apparent thermal conductivity at two specific locations within the cuticle where the neuron is located and lower thermal conductivity along the periphery of the sphere (i.e., area **3**, cf. Figure 1). Fourth, the multilayered structure was composed of alternating layers of ridges with high elastic modulus and low adhesion and grooves with lower elastic modulus and high adhesion. At elevated temperatures, interlayer areas became softer, creating an alternating compliant-stiff layered structure. Thermal expansion leads to a modest variation of interlayer periodicity with an estimated thermal expansion coefficient of 1.5×10^{-4} grad^{-1}. This value is close to the range of thermal expansion coefficients required for cuticle to possess thermal expansion to work as photomechanical sensor.[4] To clarify some details of the thermomechanical behavior of functioning biological IR receptors, more sophisticated experimental setups should be implemented to include in situ studies of the IR receptors on live beetles with minimum distortions introduced by the preparation procedure.

Considering the role of our microstructural findings for understanding of the IR receptor behavior and prospective biomimetic design, we could make some additional remarks. We can speculate that the lamellated structure of the endocuticle present in the peripheral area of the sphere along with sphere dimensions within the IR wavelength range may be critical elements designed by nature for high thermal sensitivity of the biological IR receptors. Thermal processes are inherently slow compared to photonic processes.[21] However, multilayered design would provide the advantages of speed and sensitivity within the pit organ. By analogy to a camera iris, which is multilayered, it is quicker to move several smaller objects than one large object. Nature might be implementing this design, i.e., multilayered outer shells, that reduce the time constant of a thermal process. Lowering the mass of responding elements decreases the inertial threshold thus decreasing the response time. On the other hand, sphere dimension in the micrometer range may help them to serve as "microresonators" to enhance adsorption of the IR irradiation.

From the point of view how these receptors can monitor thermal flux, their design to some extent recall the design of Golay cells that is based on the detection of a submicrometer scale deviation of thin membranes caused by expanded gas in a sealed cell.[21−23] This design showed much improved sensitivity with a millisecond response time. It seems to us that several steps were undertaken by nature to increase thermal sensitivity of these receptors as compared to the Golay design. First, the outer receptor membrane is obviously composed of flexible materials with much higher compliance than solid membranes in current Golay cells. The

design of the endocuticle from very compliant thin walls should provide much higher flexibility of the structure as compared to a rigid single membrane in current Golay design. Second improvement is the multilayered structure of these walls that provides much faster response as we discussed above but also allows much higher probability for particular temperature fluctuation resulting in expansion of particular walls elements. Finally, the spherical design with multilayered structures surrounding the vertex of the receptor instead of planar membrane arrangement results in significant amplification (by a factor of 2π) of the geometrical displacements, thus increasing thermal sensitivity of the design. Obviously, testing of these suggestions goes beyond the scope of this publication. It requires extensive studies on living specimens to characterize microthermomechanical parameters and understand how this design can be transferred to a microtechnology-compatible design.

Acknowledgment. This work is supported by AFOSR, Contract F49620-98-1-0480, and DARPA, Grant F49620-98-1-0489.

References and Notes

(1) Evans, W. G. *Nature* **1964**, *202*, 211.
(2) Evans, W. G. *Ecology* **1966**, *47*, 1061.
(3) Schmitz, H.; Bleckmann, H. *J. Comput. Physiol.* **1998**, *A182*, 647.
(4) Vondran, T.; Apel, K.-H.; Schmitz, H. *Tissue Cell* **1995**, *27*, 645.
(5) French, A. S. *Annu. Rev. Entomol*. **1988**, *33*, 39.
(6) French, A. S. *Annu. Rev. Physiol.* **1992**, *54*, 135.
(7) Thurm, U. In *Neurowissenschaft*, Dudel, J., Menzel, R., Schmidt, R. F., Eds.; Springer: Berlin, Heidelberg, Germany, and New York, 1996; p 331.
(8) Tsukruk, V. V.; Reneker, D. H. *Polymer* **1995**, *36*, 1791.
(9) Tsukruk, V. V. *Rubber Chem. Technol.* **1997**, *70*, 430.
(10) Chizhik, S. A.; Huang, Z.; Gorbunov, V. V.; Myshkin, N. K.; Tsukruk, V. V. *Langmuir* **1998**, *14*, 2606.
(11) Tsukruk, V. V.; Huang, Z.; Chizhik, S. A.; Gorbunov, V. V. *J. Mater. Sci. Lett.* **1998**, *33*, 4905.
(12) Tsukruk, V. V.; Gorbunov, V. V. *Probe Microsc.*, **2001**, submitted.
(13) Tsukruk, V. V.; Huang, Z. *Polymer* **2000**, *41*, 5541.
(14) Gorbunov, V. V.; Fuchigami, N.; Tsukruk, V. V. *Probe Microsc.* **2000**, in press.
(15) Gorbunov, V. V.; Fuchigami, N.; Tsukruk, V. V. *Probe Microsc.* **2000**, in press.
(16) Hepburn, H. R. In *Comprehensive Insect Physiology Biochemistry and Pharmacology*; Kerkut, G. A., Gilbert, L. I., Eds.; Pergamon Press: Oxford, England, 1985; Vol. 3, p 1.
(17) Neville, A. C. *Biology of the Arthropod Cuticle*; Springer: Berlin, 1975.
(18) Ratner, B., Tsukruk, V. V., Eds. *Scanning Probe Microscopy in Polymers*; ACS Symposium Series 694; American Chemical Society: Washington, DC, 1998.
(19) Tsukruk, V. V., Wahl, K., Eds. *Microstructure and Microtribology of Polymer Surfaces*, ACS Symposium Series 741; American Chemical Society: Washington, DC, 2000.
(20) Schmitz, H.; Bleckmann, H.; Murtz, M. *Nature* **1997**, *386*, 773.
(21) Chapman, R. F. *The Insects*; Cambridge University Press: Cambridge, England, 1998.
(22) Golay, M. J. *Rev. Sci. Instrum.* **1947**, *18*, 357.
(23) Chevrier, J.-B.; Baer, K.; Slater, T. *J. Micromech. Microeng.* **1995**, *5*, 193.
(24) Yamashita, K.; Murata, A.; Okuyama, M. *Sensors Actuators* **1998**, *A66*, 29.

BM005648I